Mon. Not. R. Astron. Soc. **300,** 497–510 (1998)

Starlight polarization and CO observations towards the Lupus clouds

J. R. Rizzo,[1,2]⋆† R. Morras[1,3]⋆‡ and E. M. Arnal[1,3]‡§
[1] *Instituto Argentino de Radioastronomía, Casilla de Correo 5, 1894 Villa Elisa, Argentina*
[2] *National University of La Plata, Faculty of Engineering, Calles 1 y 47, 1900 La Plata, Argentina*
[3] *National University of La Plata, Faculty of Astronomy and Geophysics, Paseo del Bosque S/N, 1900 La Plata, Argentina*

Accepted 1998 June 12. Received 1998 June 8; in original form 1997 December 16

ABSTRACT

We performed an observational study of the dark filaments Lupus 1 and Lupus 4 using both polarimetric observations of 190 stars and a sample of 72 ^{12}CO profiles towards these clouds. We have estimated lower limits to the distances of Lupus 1 and Lupus 4 ($\gtrsim$ 140 and $\gtrsim$ 125 pc, respectively). The observational strategy of the survey allows us to compare the projected magnetic field in an extended area around each cloud with the magnetic field direction observed to prevail along the clouds. Lupus 4 could have collapsed along the magnetic field lines, while in Lupus 1 the magnetic field appears to be less ordered, having the major axis of the filaments parallel to the large-scale projected magnetic field. These differences would imply that both filaments have different pattern evolutions. From the CO observations we have probed the velocity fields of the filaments and the spatial extension of the molecular gas with respect to the dust.

Key words: polarization – ISM: clouds – dust, extinction – ISM: individual: Lupus – ISM: magnetic fields – radio lines: ISM.

1 INTRODUCTION

The Lupus star-forming region is a group of dark clouds surrounding a great number of T Tauri stars (Krautter 1991). It is one of the largest T associations of the southern sky, stretching over at least 23° perpendicular to the Galactic plane, and represents one of the nearest low-mass star-forming regions.

The T Tauri stars are concentrated in four subgroups designated Lupus 1 to Lupus 4 (Schwartz 1977). The Lupus 1 and Lupus 2–4 subgroups are associated with small dark clouds which are embedded in a large complex of CO emission (Murphy, Cohen & May 1986). Besides T Tauri stars, other peculiar stellar objects have been found in these clouds, namely one Herbig Ae/Be star and a few Herbig–Haro objects. These findings are indicative of a very recent episode of star formation (10^5–10^6 yr ago). Very recently Krautter et al. (1997), using *ROSAT* observations, have found a population of 'weak-line' T Tauri stars, which apparently are not correlated with the most obscured zones of the region.

Krautter (1991) has reviewed the properties of the Lupus clouds and their related young objects. He claims that the mass spectrum of the T Tauri stars is rather unusual, suggesting that its initial mass function differs from those in other well known T associations like the Taurus–Auriga complex. He suggests as a possible explanation that the star formation in Lupus might be supported against gravitational collapse by the ambient magnetic field. Shu, Adams & Lizano (1987) proposed that magnetic field support leads to low star-formation efficiency and that, in the *subcritical* regime, if the magnetic forces exceed the gravitational ones, low-mass stars should preferentially be formed. From their polarization measurements, Strom, Strom & Edwards (1988) suggested that the Lupus 1 cloud has probably been forced to collapse along the magnetic field lines, which may have played a major role in controlling the properties of the protostellar cores.

Measurements of light polarization from stars that are either embedded in, or located beyond, a dark cloud can be used to map the geometry (projected on to the plane of the sky) of the magnetic field in the cloud, assuming that the polarization is mainly caused by non-spherical dust grains in the cloud aligned by the magnetic field (Davis & Greenstein 1951). Several efforts have been made to understand the patterns of the projected magnetic fields, as derived from starlight polarization measurements, that are likely to be associated with elongated dark clouds (Vrba, Strom & Strom 1976; Heyer et al. 1987; Goodman et al. 1990; Arnal, Morras & Rizzo 1993). In most cases, it looks as if the interstellar magnetic field plays an important role in determining the evolution of the molecular cloud.

As pointed out by Heiles et al. (1993), polarization maps of clouds presented in isolation and removed from their environments may be misleading for correlations or alignments found within a given cloud. However, these features might not be peculiar to the

⋆Visiting astronomer at Complejo Astronómico El Leoncito, which is operated under an agreement between the Consejo Nacional de Investigaciones Científicas y Técnicas de la República Argentina (CONICET), the Secretaría de Ciencia y Tecnología de la Nación and the National Universities of La Plata, Córdoba and San Juan.
† Fellow of CONICET.
‡ Member of the Carrera del Investigador Científico of CONICET.
§ Visiting astronomer at Cerro Tololo Interamerican Observatory, Chile.

cloud itself. Instead, they might characterize not only the cloud but also the region where it is embedded. For example, individual clouds in Ophiuchus and Taurus which appear to be 'parallel' or 'perpendicular' to the magnetic field (Goodman et al. 1990; Heyer et al. 1987), when their magnetic field orientations are compared with large-scale polarization maps of their surroundings, it is found that the cloud orientation may be fortuitous, because of the bias of optical polarization which probes the visually absorbing gas located at the periphery of the cloud (Heiles et al. 1993). Thus, it is advisable to observe a sample of stars located at different angular distances from the cloud, and spread over a large area around it.

In this paper we present the results of an observational study of Lupus 1 and Lupus 4. Both clouds show signs of internal fragmentation into globule-like beads. A small globule seen in projection close to Lupus 4 was also observed. These clouds are included in the Catalogue of Dark Globular Filaments (GF) of Schneider & Elmegreen (1979) and are identified as GF19 (Lupus 1), GF17 (Lupus 4) and GF18 (the globule). These authors found that the opacity, measured in visual extinction units on the Lynds (1962) scale, ranges from 5 to 6 for Lupus 1 and between 4 and 6 for Lupus 4. Maps of the distribution of visual extinction in these clouds can be found in Andreazza & Vilas-Boas (1996). Formaldehyde, in the $l_{10} \rightarrow l_{11}$ rotational transition at 6 cm, was detected in absorption in these clouds by Sandqvist & Lindroos (1976). Similar observations toward Lupus 4 were also carried out by Goss et al. (1980).

The observational material comes from polarimetric observations of both stars projected on the sky on the outskirts of the dark clouds and stars shining through the less obscured part of the clouds, together with ^{12}CO 115-GHz observations towards both filaments and their environments. The relationship between the magnetic field geometry and the dark cloud morphology may provide important clues about the most likely scenarios for the cloud evolution. The velocity field of both clouds was mapped by observing the ^{12}CO ($J = 1 \rightarrow 0$) transition. Since the gas and the dust are mixed, observations of polarization of stars with known distances could also be used to estimate a lower limit on the distances to the molecular clouds.

2 OBSERVATIONS

2.1 Optical polarimetry

The polarimetric measurements were performed using the Vatican Polarimeter (VATPOL) mounted at the Cassegrain focus of the 2.15-m telescope at El Leoncito (CASLEO, Argentina). A thorough description of the VATPOL system was provided by Magalhaes, Benedetti & Roland (1984). The observations were carried out in two observing runs during 1991 June and 1992 June, respectively. Unfiltered, linear optical polarization measurements were obtained for 190 programme stars, which were selected on the basis of both their apparent brightness and their angular distance from Lupus 1 and Lupus 4. From this sample, 40 and 46 weak stars are seen projected on to the dust patches delineating Lupus 1 and Lupus 4, respectively. A total of 66 and 38 'field stars', that is to say stars located away from the dark clouds, were observed on the outskirts of Lupus 1 and Lupus 4, respectively. The position angle zero-point and instrumental polarization values were established by regularly observing a sample of highly polarized and nearby unpolarized standard stars, respectively. The instrumental polarization was found to be less than 0.03 per cent.

2.2 Carbon monoxide

Observations of the 2.6-mm line ^{12}CO $J = 1 \rightarrow 0$ were made with the 1.2-m Columbia Millimeter-Wave Telescope at Cerro Tololo, Chile, during 1985 January. At the CO frequency (115.2712 GHz) the radio telescope has an angular resolution (FWHM) of ≈ 8.7 arcmin. A 256-channel filter bank of 100 kHz bandwidth per channel was used at the back end. The velocity resolution was 0.26 km s^{-1}, and the velocity coverage ≈ 66 km s^{-1}. A detailed description of the instrument was given by Cohen (1983). The observational method, reduction and calibration of the profiles were similar to those used by Arnal et al. (1993). Typical final rms noise per profile was of the order of $\sim$0.27 K.

A total of 41 points in Lupus 1 and 31 points in Lupus 4 were observed.

3 RESULTS

3.1 Optical polarimetry

The results of the observations of the 190 programme stars are given in Tables 1 and 2, respectively. In Table 1 the observational results corresponding to those stars seen in projection on to, or close to, the filamentary globules are given. A star sequence identification number is given in the first column. The observed percentage polarization P, its probable error $\epsilon(P)$, the position angle of polarization θ (in degrees), and its error $\epsilon(\theta)$ are given in the second, third, fourth and fifth columns, respectively. The position angles θ are measured east of north and the uncertainty in θ is given by the formula $\epsilon(\theta) = 28\overset{\circ}{.}65\ [\epsilon(P)/P]$ (Serkowski 1974). In Table 2, the results corresponding to the so-called 'field stars' are provided. There, the star HD and SAO number are given in the first and second columns, respectively. The corresponding P, $\epsilon(P)$, θ and $\epsilon(\theta)$ are given in the third, fourth, fifth and sixth columns, respectively. In the seventh column, when available, the visual magnitude is listed, as quoted in the SAO Catalogue. In the eighth column the spectral type according to the Michigan Catalogue (Houk & Cowley 1975) is listed. The numbers 1 or 4 quoted in the ninth column indicate the field to which the star belongs (Lupus 1 or Lupus 4).

Finding charts for the stars observed in the central parts of Lupus 1 and Lupus 4 are given in Figs 1(a) and (b), respectively. The dark clouds are clearly visible in the charts as well-defined dark lanes. The positions of the observed stars are indicated according to the number assigned in Table 1. In Figs 2(a) and (b) the polarization vectors of these stars have been drawn. The length of the polarization vector is proportional to P and it is oriented in the direction indicated by θ. In Fig. 3 polarization vectors of the 104 'field stars' are plotted together. In Figs 2(b) and 3, polarizations lower than 0.5 per cent are indicated by an open circle.

3.2 CO observations

3.2.1 *Lupus 1*

In Fig. 4 the observed CO positions, marked by filled circles, along with a small but representative sample of CO profiles, are shown. The selected CO profiles are depicted inside rectangular boxes. A straight line joins every box with the actual observed position. Solid con tour lines corresponding to the visual absorption map of Andreazza & Vilas-Boas (1996) are also shown, to help the reader to pin down regions of high optical obscuration. Those positions observed at the H_2CO 6-cm line by Sandqvist & Lindroos (1976) are indicated by open squares. Most of the profiles are

Table 1. Polarimetric observations of weak stars in Lupus 1 and Lupus 4.

Lupus 1

Star Nr.	P	$\epsilon(P)$	θ	$\epsilon(\theta)$	Star Nr.	P	$\epsilon(P)$	θ	$\epsilon(\theta)$	Star Nr.	P	$\epsilon(P)$	θ	$\epsilon(\theta)$
1	2.50	0.36	36.4	4.1	15	1.34	0.23	36.1	4.9	28	1.99	0.44	81.6	6.3
2	2.60	0.20	42.5	2.2	16	0.85	0.34	37.0	11.5	29	1.08	0.14	46.9	3.6
3	1.88	0.53	53.2	8.1	17	0.81	0.08	62.3	2.9	30	1.31	0.20	56.8	4.3
4	0.72	0.15	170.0	5.9	18	1.24	0.19	37.0	4.5	31	2.47	0.19	71.1	2.2
5	1.35	0.10	108.8	2.2	19	0.90	0.10	47.3	3.2	32	0.70	0.13	59.2	5.5
6	2.11	0.25	44.2	3.4	20	0.95	0.17	50.7	5.2	33	1.41	0.14	34.6	2.8
7	1.71	0.42	91.0	7.0	21	2.54	0.27	72.1	3.1	34	2.23	0.14	30.5	1.8
8	1.62	0.23	27.6	4.1	22	2.00	0.35	32.1	5.0	35	1.80	0.16	80.1	2.6
9	0.71	0.10	58.9	4.0	23	2.46	0.16	34.3	1.9	36	1.15	0.11	58.9	2.7
10	1.43	0.27	42.7	5.3	24	2.08	0.18	70.5	2.5	37	2.15	0.33	77.5	4.4
11	0.84	0.13	57.1	4.3	25	0.93	0.13	77.5	3.9	38	1.29	0.07	70.2	2.2
12	1.24	0.20	4.9	4.5	26	1.07	0.11	73.3	3.0	39	1.11	0.51	51.1	13.2
13	2.19	0.29	52.1	3.8	27	0.96	0.14	12.1	4.1	40	1.19	0.14	70.3	3.5
14	1.80	0.13	63.2	2.1										

Lupus 4

Star Nr.	P	$\epsilon(P)$	θ	$\epsilon(\theta)$	Star Nr.	P	$\epsilon(P)$	θ	$\epsilon(\theta)$	Star Nr.	P	$\epsilon(P)$	θ	$\epsilon(\theta)$
1	2.51	0.07	22.3	0.8	17	3.02	0.29	22.9	2.7	32	3.84	0.18	37.9	1.3
2	0.04	0.06	–	–	18	3.00	0.48	20.9	4.6	33	3.22	0.20	30.8	1.8
3	4.32	0.56	31.5	3.7	19	3.48	0.53	32.6	4.3	34	2.63	0.28	29.7	3.1
4	5.26	0.20	20.8	1.1	20	3.86	0.32	32.5	2.3	35	2.31	0.22	29.8	2.7
5	4.06	0.13	14.8	0.9	21	4.43	0.26	31.7	1.7	36	1.42	0.16	24.3	3.2
6	4.60	0.22	13.4	1.4	22	2.98	0.27	32.4	2.5	37	1.67	0.18	19.0	3.1
7	4.20	0.22	9.4	1.5	23	3.33	0.32	32.1	2.7	38	0.93	0.17	22.6	5.2
8	3.76	0.32	23.7	2.4	24	4.12	0.46	46.7	3.2	39	3.08	0.14	18.3	1.3
9	4.55	0.49	24.7	3.1	25	2.68	0.20	32.6	2.2	40	5.28	0.32	27.9	1.7
10	3.33	0.50	20.9	4.3	26	4.01	0.35	35.3	2.5	41	2.66	0.14	28.1	1.5
11	1.53	0.15	4.2	2.8	27	4.17	0.50	34.3	3.5	42	5.99	0.67	34.4	3.2
12	0.48	0.15	10.3	9.2	28	1.88	0.27	23.0	4.1	43	2.53	0.20	14.6	2.3
13	5.02	0.28	27.1	1.6	29	0.93	0.17	22.6	5.2	44	3.59	0.22	38.5	1.7
14	4.51	0.34	14.7	2.1	30	1.82	0.27	34.8	4.2	45	3.82	0.16	24.0	1.2
15	1.08	0.42	46.1	11.2	31	3.37	0.15	36.6	1.3	46	4.61	0.13	35.8	0.8
16	5.00	0.27	21.5	1.6										

single-peaked and exhibit velocity asymmetries. No clear correlation between the line asymmetries and the location of observed points has been found. A few of these profiles, three out of 41, show a clear double-peak structure. All profiles are broad (FWHM up to 3.2 km s^{-1} are observed, the average being 2.3 km s^{-1}) and the peak temperature over the filament reaches $\sim$ 8 K. Table 3(a) summarizes the observed line parameters: the first column gives a profile number; the second and third columns correspond to the equatorial coordinates (1950.0) of the observed point; the observed peak brightness temperature ($T_{\rm max}$), the mean temperature-weighted radial velocity ($V_{\rm R}$) and the line integral ($W_{\rm CO}$) are listed in the fourth, fifth and sixth columns, respectively. Omitted parameters correspond to those points having $T_{\rm max}$, or $W_{\rm CO}$, values lower than 3 times the rms noise. The $W_{\rm CO}$ along the filament has a clear decreasing trend from north-west to south-east.

3.2.2 Lupus 4

The main observational results for this cloud are summarized in Table 3(b). The meaning of the columns is similar to that in Table 3(a). We include for this region the CO observations of both Lupus 4 and the globule GF18. Due to a lack of observing time, no CO data were obtained outside the optical borders of the globule.

We present a montage of several of the observed CO profiles in Fig. 5. As in Fig. 4, we also have superimposed the visual absorption contours of Andreazza & Vilas-Boas (1996). All the CO profiles are single-peaked with mean FWHM values of 1.23 and 1.44 km s^{-1} for Lupus 4 and GF18, respectively. Peak temperatures are 7–8 K over Lupus 4 and 4–6 K over GF18. The radial velocities ranges between 4 and 5 km s^{-1} and 3 and 4 km s^{-1} for Lupus 4 and GF18, respectively.

The profiles in Lupus 4 are narrower and more similar to each other than those of Lupus 1. However, systematic profile asymmetries at positive velocities are present in almost all of them.

4 DISCUSSION

4.1 Cloud distances

Based on the spectroscopic information available for the 'field stars' (those listed in Table 2), an individual distance modulus, not corrected for extinction, was derived for every star of known spectral type. We could not obtain its counterpart for those stars observed in projection on to, or located at a small angular distance from, the clouds (those stars listed in Table 1), because photometric and spectroscopic information about them is lacking.

Since there is no available *UBV* photometry for most of the 'field stars', except for a few of the brightest and nearest ones, following Morras (1981) and Arnal et al. (1993), a lower limit to the visual extinction was estimated using the relationship $P_{\rm V} \leq 3A_{\rm V}$ (Hiltner 1956).

Table 2. Polarimetric observations towards field stars in the Lupus 1 and Lupus 4 regions.

HD	SAO	P (%)	ε(P) (%)	θ (°)	ε(θ) (°)	m_v	ST	Field
138089	206718	0.04	0.06	50.4	37.0	8.0	F0V	1
138491	206754	0.65	0.03	144.4	1.3	8.0	A5V	1
138529	206762	0.51	0.05	15.5	2.6	8.6	G8/K0III	1
138575	206768	0.14	0.06	156.3	12.0	7.1	A0V	1
138617	206777	0.66	0.04	124.5	1.9	8.2	K0III	1
138924	206797	0.13	0.04	132.3	8.9	8.3	F7V	1
138994	206803	0.13	0.08	70.2	19.0	8.2	F2V	1
139011	206805	0.06	0.06	47.0	32.0	8.9	F8V	1
139095	206810	0.08	0.03	152.8	10.0	8.0	A9/F0V	1
139124	206813	0.13	0.45	133.9	104.0	8.6	F2V	1
139450	206837	0.14	0.04	151.4	7.7	8.7	G0/1V	1
139522	206847	0.05	0.05	89.4	33.0	7.9	F2V	1
139542	206846	0.08	0.05	173.7	19.0	8.8	F3V	1
139676	206863	0.04	0.07	17.6	44.0	7.6	A9V	1
139696	206864	0.05	0.06	108.6	34.0	8.7	K3V	1
139766	206868	0.52	0.05	130.7	2.9	8.7	A7/8V	1
139883	206877	0.11	0.04	105.0	10.0	8.4	F2V	1
139979	206886	0.09	0.06	175.2	19.0	8.4	F0V	1
140056	206894	0.47	0.07	149.1	4.5	10.0	A8/9V	1
140075	206895	1.49	0.06	129.4	1.1	8.7	A5/7II	1
140076	206896	0.22	0.03	131.3	3.7	8.8	F3V	1
140195	206908	0.92	0.05	135.1	1.5	9.2	B9.5V	1
140304	206918	0.63	0.03	129.8	1.6	7.8	K4III	1
140330	206922	0.62	0.04	110.8	1.8	8.3	M0III	1
140391	206926	0.04	0.05	19.7	39.0	8.3	F3V	1
140462	206929	0.55	0.03	113.1	1.6	8.9	K4III	1
140495	206933	0.08	0.07	40.0	25.0	9.1	F3V	1
140497	206934	1.03	0.05	120.9	1.4	9.2	A9/F0V	1
140601	206944	0.58	0.06	124.7	3.1	9.1	AOV	1
140703	206955	0.03	0.04	139.3	47.0	8.2	F3V	1
140757	206964	0.11	0.08	113.1	20.0	8.2	A2IV/V	1
140940	206978	0.02	0.05	65.1	74.0	8.7	F7/8V	1
140973	206991	0.04	0.03	50.3	19.0	7.3	F5/7II	1
141050	206993	0.94	0.04	133.1	1.2	8.7	K1III	1
141109	206998	0.57	0.05	153.5	2.5	8.4	K0III	1
141110	206999	1.18	0.07	128.6	1.8	9.4	F2V	1
141191	—	0.71	0.06	25.7	2.4	—	F2IV	1
141294	207016	0.09	0.07	169.2	22.0	9.1	F5V	1
141327	207020	0.17	0.06	14.7	11.0	7.4	B9V	1
141361	207021	0.56	0.04	125.5	2.2	8.6	K1III	1
141518	207034	0.06	0.05	10.0	26.0	8.5	F3V	1
141519	207038	0.19	0.05	2.3	7.9	9.4	A1IV	1
141536	207039	0.08	0.04	110.1	16.0	8.5	F3V	1
141643	207048	0.10	0.05	104.8	14.0	7.1	K3III	1
141759	207060	0.02	0.08	134.8	131.0	9.2	F5V	1
141801	—	2.59	0.04	123.7	0.4	—	F5V	1
141815	207065	0.09	0.05	179.2	17.0	7.6	F7V	1
141978	207083	1.14	0.04	120.9	1.0	9.9	G5V	1
141998	207085	3.06	0.05	130.4	0.5	9.3	A9V	1
142017	207087	0.28	0.05	54.5	5.8	9.0	F3V	1
142041	207088	0.06	0.09	1.3	42.0	9.2	A8/9V	1
142116	226328	1.88	0.03	156.7	0.5	9.5	B9III/IV	4

HD Nr.	SAO Nr.	P (%)	ε(P) (%)	θ (°)	ε(θ) (°)	m_v	ST	Field
142187	207100	0.08	0.11	101.3	40.0	9.0	F6V	1
142254	226361	0.06	0.06	135.1	30.0	6.8	F3V	4
142275	207107	0.09	0.05	90.3	18.0	9.1	F3V	1
142276	207108	1.93	0.03	115.7	0.4	9.7	A9V	1
142302	207112	0.30	0.03	6.5	2.7	9.7	A5III	4
142317	207110	0.64	0.07	155.1	3.3	9.0	A0V	1
142318	207115	1.77	0.05	126.6	0.8	10.0	A2/3III	1
142426	207121	1.34	0.04	122.4	0.9	9.5	F5V	1
142448	207128	1.27	0.04	14.4	0.9	8.2	B9V	4
142484	207132	0.38	0.06	81.1	4.9	9.1	A0V	1
142558	207138	0.59	0.05	100.6	2.2	8.9	K0III	1
142643	207146	0.12	0.06	99.5	14.0	7.0	A3V	1
142786	207160	1.01	0.09	113.2	2.6	9.1	A9V	1
142832	207170	1.90	0.05	123.0	0.7	9.5	F3V	1
142852	226415	0.06	0.05	4.3	28.0	8.2	A6V	4
143009	226425	0.08	0.04	33.4	12.0	5.0	G8III	4
143097	207201	2.47	0.04	137.2	0.5	9.3	G8II/III	1
143149	207205	0.07	0.06	175.9	22.0	7.0	A0V	1
143151	226436	3.47	0.07	161.2	0.6	9.5	B9V	4
143281	—	1.06	0.02	28.4	0.6	—	F0V	4
143337	207230	0.13	0.07	152.8	16.0	8.0	G3V	1
143404	207234	0.26	0.04	125.5	4.6	6.4	K4III	1
143463	226457	0.04	0.06	129.7	38.0	7.2	F6V	4
143561	226463	2.09	0.04	3.5	0.6	7.5	G8III	4
143602	—	3.91	0.11	141.6	0.9	—	K1/2(III)	4
143792	226472	2.10	0.06	6.3	0.9	8.0	B9V	4
143880	—	0.76	0.04	149.4	1.4	—	F5V	4
143904	226484	2.02	0.03	167.4	0.5	9.6	A0V	4
143980	—	1.38	0.04	5.0	0.9	—	F8/G1	4
144007	—	3.67	0.10	153.5	0.8	—	K2(III)	4
144196	226502	0.84	0.04	174.9	1.4	9.5	F3V	4
144277	207329	0.05	0.04	42.0	20.0	8.0	A1V	4
144296	226510	1.15	0.05	157.8	1.2	8.5	A3V	4
144350	226517	0.42	0.05	2.1	3.2	7.3	K2/3III	4
144552	226527	0.90	0.04	19.5	1.2	8.5	K1III	4
144572	226529	0.64	0.03	159.7	1.4	9.0	F5V	4
144884	226547	2.32	0.04	153.4	0.5	9.0	A0V	4
145173	207423	0.07	0.04	5.8	16.0	7.9	F5V	4
145191	226564	0.02	0.04	41.0	54.0	6.2	F2III+A	4
145510	226580	0.04	0.04	177.4	24.0	7.6	FOIV	4
145903	226601	0.06	0.06	137.4	28.0	9.5	F5V	4
145921	226603	0.09	0.04	25.3	13.0	6.2	K2III	4
145983	226606	1.82	0.05	154.9	0.8	9.7	B7Ib/II	4
145984	226608	0.02	0.05	15.6	73.0	9.0	F2V	4
146057	226612	0.85	0.05	10.3	1.5	6.9	K1III	4
146221	226622	1.44	0.03	5.6	0.5	10.0	A0V	4
146301	226627	1.27	0.06	63.2	1.2	8.5	F2IV	4
146458	226637	0.25	0.09	131.4	10.0	9.0	F6V	4
146681	226651	1.11	0.09	23.5	2.2	8.9	A7II/III	4
146777	226661	0.63	0.03	13.0	1.5	9.7	A3II/III	4
146882	226669	0.14	0.07	4.6	13.0	8.7	F6V	4
147271	226701	2.07	0.06	27.7	0.9	9.0	A2III/IV	4

(a)

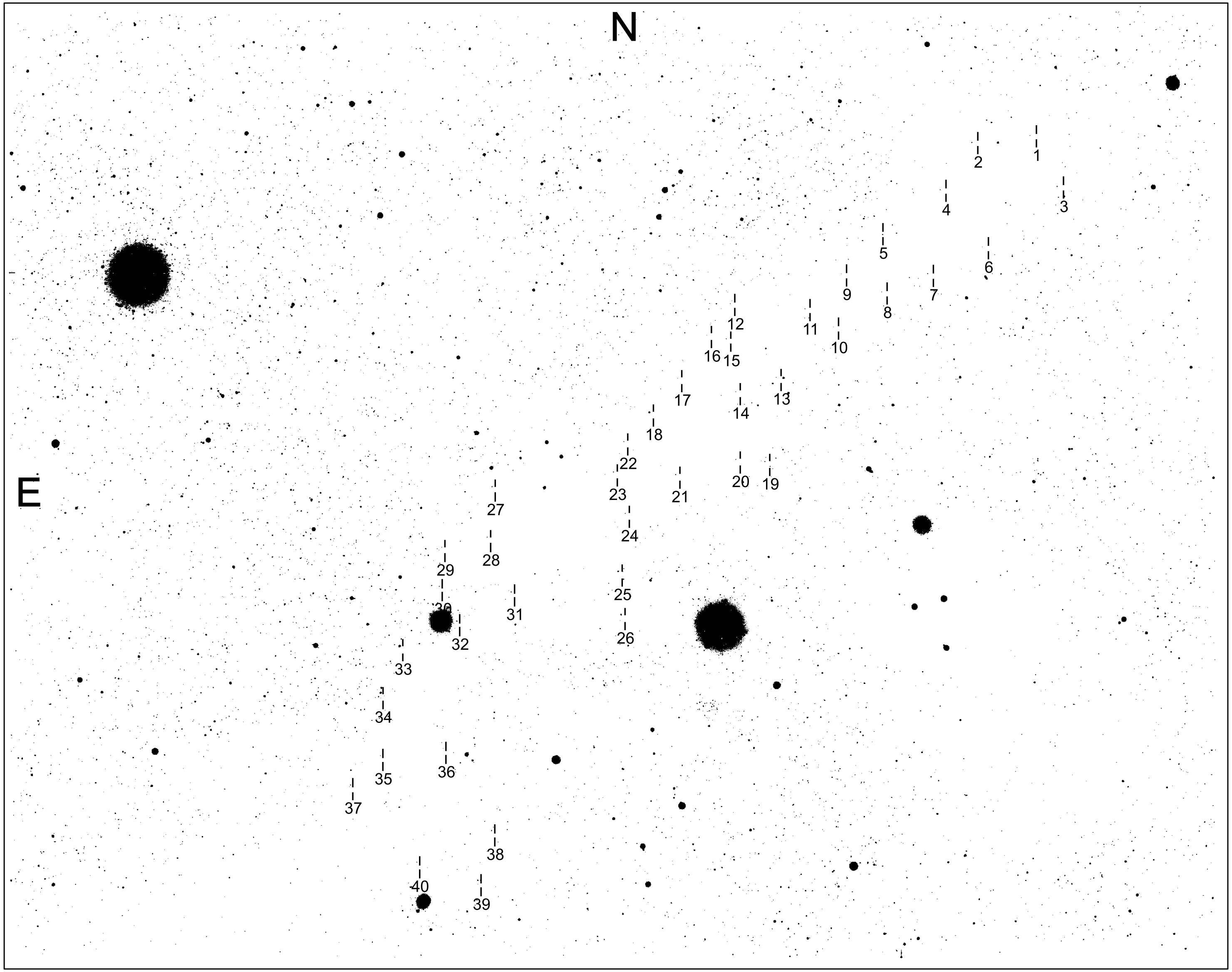

Figure 1. (a) Finding chart of the weak stars observed in the Lupus 1 field. The plate was taken from the double 20-inch astrographic telescope of the astronomical station Dr Carlos U. Cesco, operated under agreement between the Félix Aguilar Observatory, San Juan, Argentina, and the Yale Southern Observatory. The emulsion of the plate is Kodak 103a-0. The positions of the observed stars are indicated with numbers assigned according to Table 1. Equatorial coordinates (1950.0) of the centre are RA = $15^{h}41^{m}00^{s}$ and Dec. = $-34°05'02''$. (b) The same as (a) for the weak stars observed in the Lupus 4 field. Equatorial coordinates (1950.0) of the centre are RA = $16^{h}00^{m}00^{s}$ and Dec. = $-41°55'02''$.

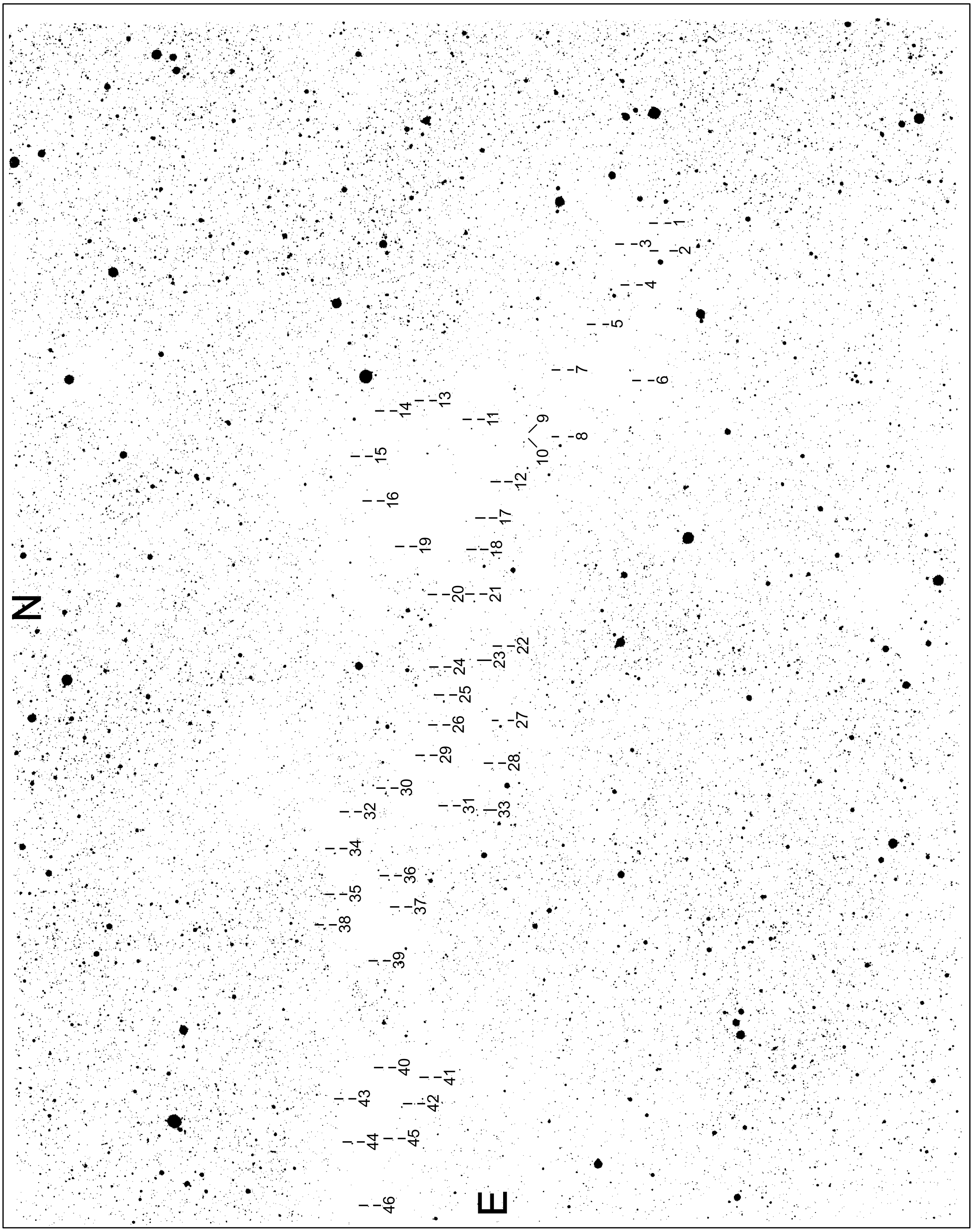

(b)

Figure 1 – *continued*

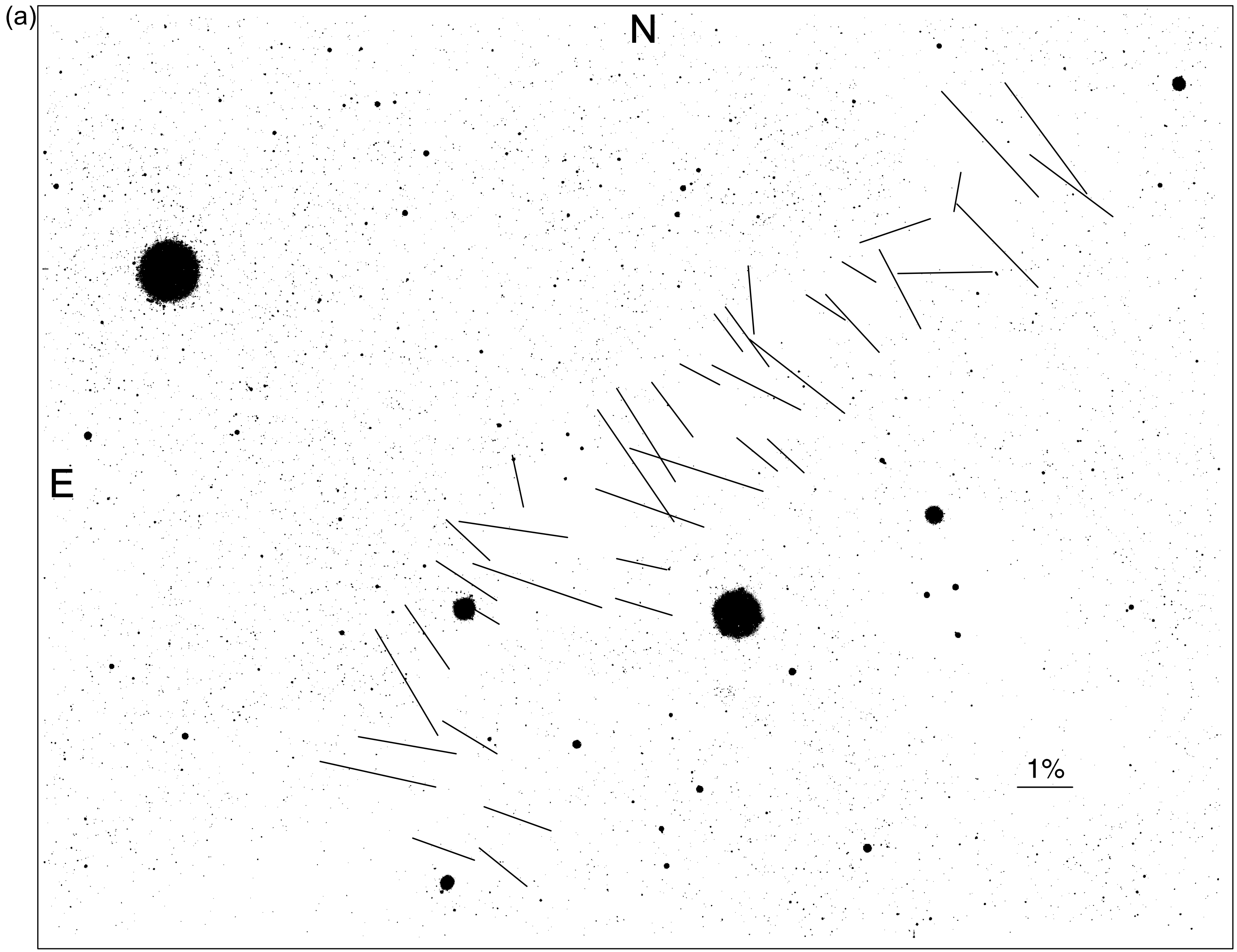

Figure 2. (a) Polarization vectors corresponding to the sample of weak stars close to Lupus 1. The lengths of the *E*-vectors are proportional to the percentage of linear polarization observed. They are centred at the positions of the observed stars. (b) The same as (a), for the weak stars observed in the Lupus 4 field. Open circles represent stars having a percentage polarization lower than 0.5 per cent. The vector corresponding to the star 46 was not drawn because it would be located outside the left border of the chart.

(b)

Figure 2 – *continued*

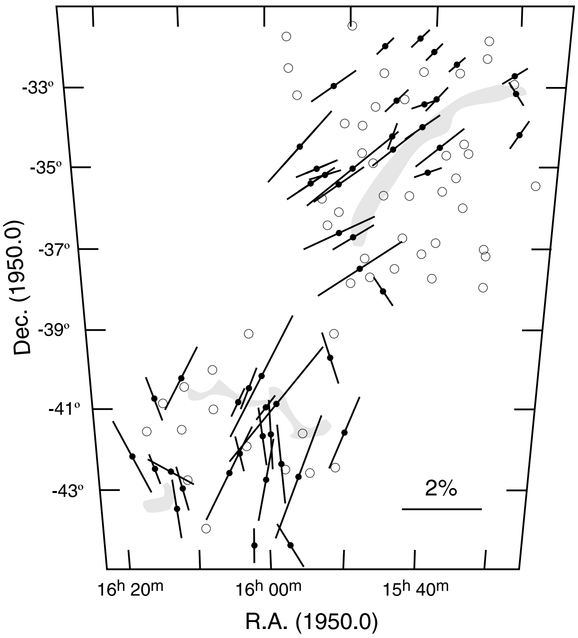

Figure 3. Polarization vectors corresponding to the sample of 'field stars', also listed in Table 2. *E*-vectors are plotted, proportional to the percentage of linear polarization, centred at the position of the observed stars. Open circles represent stars having a percentage polarization lower than 0.5 per cent. The grey zones indicate the positions of the dark clouds.

Then, using the absolute magnitudes listed by Corbally & Garrison (1984), a distance modulus corrected for visual extinction was obtained for every individual star. Diagrams of P_V versus this individual extinction-corrected distance modulus are shown in Figs 6(a) and (b) for stars in the fields of Lupus 1 and Lupus 4, respectively. There, a sudden increase in P_V at a distance modulus $\approx$ 5.7 mag ($\approx$ 140 pc, Fig. 6a) and 5.5 mag ($\approx$ 125 pc, Fig. 6b), respectively, is clearly noticed. We ascribed these jumps to the presence of aligned dust grains related to the molecular clouds where the dark filaments are immersed. No error bars were quoted in the individual stellar distance modulus due to a lack of true visual extinction values.

A star which appears to be in a discrepant position in Fig. 6(a) is HD 141978 (distance modulus $\approx$ 4.4 mag). It was classified as a G5V star by Houk & Cowley (1975) and they assigned to their objective-prism spectra a quality factor of 2. The latter means that *'the spectra may be slightly over- or underexposed or slightly overlapped'*. Thus, it is possible that the spectral type and/or the luminosity class could be slightly different: a small difference in the latter can mean that the distance modulus of this star will be greater (for a G5IV star, the distance modulus would roughly be 6.4 mag). Thus, its discordant position could be the result of a misclassification.

Appenzeller, Mundt & Wolf (1978) have used the bright star HD 140748, which apparently illuminates matter belonging to the molecular cloud Barnard 228, and derived a distance of 125 pc to Lupus 1. Franco (1990) have studied the colour excess distribution from stars located in the neighbourhood of Lupus 4 and found a distance of 165 $\pm$ 15 pc for this dark filament. Hughes, Hartigan & Clampitt (1993) estimated a distance of 140 $\pm$ 20 pc to the Lupus clouds, assuming that all of the Lupus subgroups are at the same distance. All these values agree well with our values of 125–140 pc, and fall within the 130–170 pc range suggested by Murphy et al. (1986). Our results and the agreement among other works would suggest that the filamentary clouds Lupus 1 and Lupus 4 are embedded in a single diffuse cloud located at a distance range of 130–170 pc.

If these estimated distances are correct, from their observed major angular sizes and their average angular widths, as determined by Schneider & Elmegreen (1979), both dark clouds are 6–7 pc long, and 0.6–0.7 pc wide.

4.2 The masses

It must be pointed out that we did not attempt to obtain the *total* molecular mass of these clouds, because the molecular gas distribution is likely to have been undersampled by our observational scheme and no information from the ^{13}CO data has been obtained. Thus, we have only used our ^{12}CO observations in order to estimate the molecular mass of *each condensation.* To do this, we selected the CO profiles located inside the condensations defined by Andreazza & Vilas-Boas (1996), namely A to F in Lupus 1 and A to D in Lupus 4. Then, we computed the total CO intensity of every condensation as

$$W_{\rm CO}^{\rm tot} = \frac{A_{\rm cond}}{A_{\rm CO}} \quad W_{\rm CO}^{\rm mean}, \tag{1}$$

where $A_{\rm cond}$ is the angular size of the condensation, as given by Andreazza & Vilas-Boas (1996) in arcmin^2, $A_{\rm CO}$ is the CO beam, (8.7 arcmin)^2, and $W_{\rm CO}^{\rm mean}$ is the average CO intensity. After this, we used the relation suggested by Strong et al. (1988) to estimate the H_2 masses of the condensations.

The obtained values are 53 (27), 6 (5), 11 (10), 15 (33), 12 (12) and 8 (8) $M_\odot$ for the condensations A to F in Lupus 1, and 2 (5), 14 (22), 4 (7) and 7 (9) $M_\odot$ for the condensations A to D in Lupus 4. The values given in brackets are the masses derived from the star counts in Andreazza & Vilas-Boas (1996).

It is very hard to determine the formal errors involved in those masses, because several sources of uncertainties are present. First, the CO/H_2 conversion factor of Strong et al. (1988), based on diffuse galactic γ-ray maps, H I surveys and CO surveys, probably has an uncertainty of $\lesssim$ 20 per cent. Although the ^{12}CO line $J = 1 \rightarrow 0$ is optically thick, this conversion factor is frequently used in the literature due to the fact that it remains at approximately the same value in different regions of the Galaxy, except towards the Galactic Centre (Ramana Murthy & Wolfendale 1993 and references therein). Secondly, the value of 3.2 assumed by Andreazza & Vilas-Boas (1996) for R_V may be another source of uncertainty: several works (Vrba & Rydgren 1984 and Arnal et al. 1993, among others) have shown that R_V increases toward the densest parts of the dark clouds.

Bearing in mind the factors mentioned above, the agreement between both estimates of the molecular masses of every individual condensation can be considered reasonable.

4.3 The ambient magnetic field

The polarization data can also be used to examine the difference between the polarization angles of those background stars, the angular distance of which from the dark clouds is small, and the polarization angles of those stars located further away (the 'field stars'). To this end, the polarization angle data, in the direction of stars with interstellar polarization greater than 0.5 per cent, were grouped into bins 10° wide, for stars observed in or close to Lupus 1 and Lupus 4 (Figs 7a–7b), and 20° wide for the so called 'field stars' (Figs 7c–7d). The mean values of the *E*-vector polarization angles θ

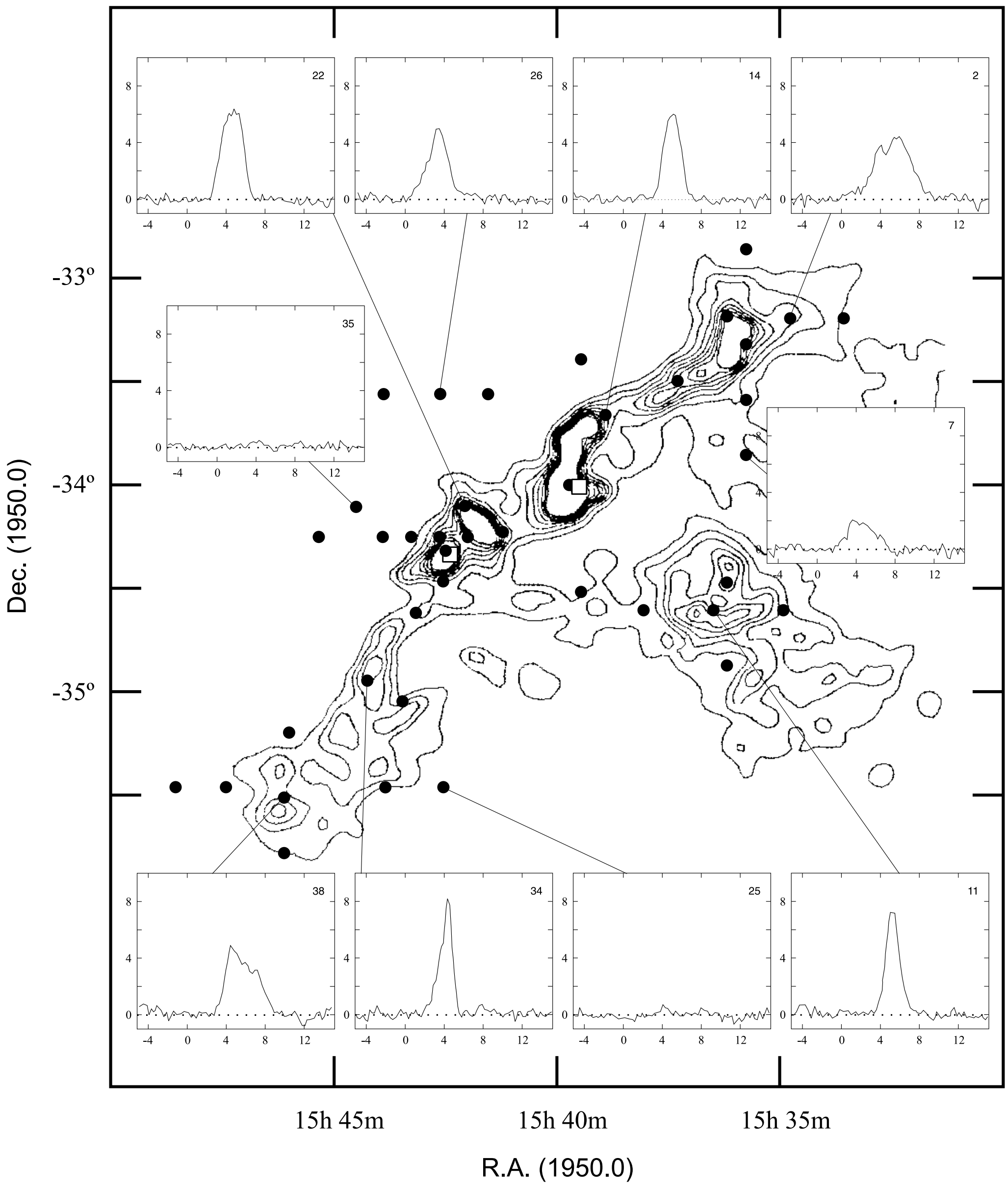

Figure 4. Montage of representative ^{12}CO profiles in the Lupus 1 region. The numbers of the profiles are referred to in Table 3(a), where exact coordinates of the positions are listed. Contour lines are from the visual absorption map of Andreazza & Vilas-Boas (1996). For the CO profiles, the plotted magnitudes are T_A^* in K (ordinates) and $V_{\rm LSR}$ in km s^{-1}. Dark points correspond to the CO observations reported in this paper, while open squares indicate the H_2CO positions observed by Sandqvist & Lindroos (1976).

and its standard deviations are given in Table 4. Myers & Goodman (1991) determine mean values for θ of 50° and 22° for Lupus 1 and Lupus 4, respectively, in good agreement with our 'close stars' values – the first and second rows of Table 4.

The observed dispersion in the polarization angle distribution is always greater than the instrumental uncertainty, suggesting that this dispersion may contain some information about the degree of variation of the magnetic field direction. A model explaining such dispersion in dark clouds, as arising from a three-dimensional magnetic field having uniform and non-uniform parts, can be found in Myers & Goodman (1991). Unfortunately, we can not apply this model to our observations, because information about the line-of-sight component of the magnetic field is not available.

In the case of Lupus 4 we note – after a visual inspection of Figs 2(b), 3 and 7, and comparing the results of Table 4 – that the projected magnetic field mean angle is very similar in both sets of data ('field stars' and 'close stars'), which suggests an alignment of the overall magnetic field roughly perpendicular to the optical filament. This observational finding allows us to suggest that Lupus 4 could have been formed as the result of matter collapse along the magnetic field lines.

The picture in Lupus 1, however, appears more complicated. Apparently, the role played by the magnetic field in controlling the properties of the dark filament is not as simple as Strom et al. (1988) suggested. Our data show that the magnetic field direction deduced from stars close to Lupus 1 is significantly different from the magnetic field direction determined from the 'field stars' data. The position vectors of the 'field stars' are remarkably well aligned with each other and with the projected long axis of the cloud (see Fig. 3), while the distribution of θ near the filament is not well

Table 3. (a) Observational CO parameters in Lupus 1. (b) Observational CO parameters in Lupus 4.

(a)

Profile	RA - 15^h (min)	Dec. (deg)	T_{max} (K)	V_{LSR} (km s^{-1})	W_{CO} (K km s^{-1})
1	33.58	−33.1975	0.71	5.03	3.241
2	34.78	−33.1975	4.20	5.47	14.83
			1.54	3.23	3.36
3	34.93	−34.6030	4.69	5.64	10.34
4	35.77	−32.8642	–	–	–
5	35.77	−33.3225	6.84	5.77	23.12
6	35.77	−33.5892	2.93	5.37	7.24
7	35.77	−33.8558	2.01	4.10	6.80
8.	36.19	−33.1975	8.11	6.22	23.15
9	36.20	−34.4697	7.09	5.36	15.37
10	36.20	−34.8692	2.67	5.34	8.13
11	36.50	−34.6030	7.56	4.86	12.43
12	37.30	−33.4989	5.15	4.96	13.68
13	38.06	−34.6030	5.87	4.93	9.64
14	38.92	−33.6625	6.25	4.69	12.81
15	39.47	−33.3948	–	–	–
16	39.47	−34.0125	6.20	5.07	13.25
17	39.47	−34.5142	4.99	4.78	10.60
			0.92	2.38	1.99
18	39.50	−34.0000	6.29	5.08	12.77
19	41.21	−34.2267	7.34	4.65	15.58
20	41.55	−33.5614	0.74	3.04	0.58
21	42.00	−34.2508	6.87	4.04	16.87
22	42.07	−34.1008	6.67	4.38	16.62
23	42.50	−34.3167	7.11	4.10	13.96
24	42.55	−34.4642	7.80	4.44	15.70
25	42.55	−35.4558	–	–	–
26	42.62	−33.5614	4.71	3.12	12.12
27	42.64	−34.2508	7.69	4.00	17.13
28	43.16	−34.6158	7.25	4.20	11.44
29	43.27	−34.2508	5.41	4.08	13.08
30	43.46	−35.0419	6.53	4.03	12.29
31	43.85	−35.4558	1.08	4.36	1.96
32	43.88	−33.5614	1.57	1.96	2.25
			2.56	0.17	5.10
33	43.90	−34.2508	1.94	3.92	4.73
34	44.25	−34.9419	7.85	4.20	10.74
35	44.50	−34.1050	–	–	–
36	45.34	−34.2508	–	–	–
37	46.00	−35.1925	3.78	4.48	6.65
38	46.12	−35.5058	4.41	5.21	17.03
39	46.12	−35.7725	–	–	–
40	47.42	−35.4558	1.60	5.77	5.54
41	48.55	−35.4558	2.33	6.56	6.29
			1.04	3.94	1.74

(b)

Profile	RA - 16^h (min)	Dec. (deg.)	T_{max} (K)	V_{LSR} (km s^{-1})	W_{CO} (K km s^{-1})
1	−7.73	−42.1375	–	–	–
2	−5.96	−42.4542	6.03	4.40	8.03
3	−4.90	−42.4542	6.24	4.67	8.25
4	−4.40	−42.2861	7.13	4.48	6.85
5	−3.60	−42.1992	6.41	4.42	7.25
6	−3.45	−42.4408	6.00	4.63	6.55
7	−2.23	−41.8875	7.48	4.03	9.19
8	−2.23	−41.6875	6.87	3.99	9.35
9	−1.70	−41.7875	7.70	3.99	11.68
10	−1.24	−41.6875	5.95	3.82	9.53
11	−0.88	−41.5361	6.98	4.09	9.27
12	−0.32	−41.8528	8.48	4.08	10.99
13	0.67	−41.8583	8.17	4.07	9.80
14	1.50	−41.8583	8.07	4.10	8.27
15	2.36	−41.6875	7.76	4.36	9.83
16	3.83	−41.4889	6.10	4.94	6.00
17	4.80	−41.4750	6.10	4.74	7.51
18	4.80	−41.6458	7.56	4.83	9.89
19	7.29	−44.5561	2.81	3.14	2.34
20	7.70	−41.6875	7.29	4.84	12.86
21	7.70	−41.7222	5.34	4.89	10.07
22	9.98	−43.9311	7.01	3.55	9.44
23	10.45	−43.7728	4.78	3.56	4.66
24	10.93	−43.2617	1.31	3.50	–
25	10.93	−43.9311	6.68	3.84	10.34
26	10.93	−44.2617	2.74	3.62	5.36
27	10.93	−44.7617	1.07	3.93	3.44
28	11.40	−43.7617	4.61	3.46	4.22
29	11.80	−43.9886	6.24	4.09	11.52
30	12.26	−43.8436	3.64	3.64	3.61
31	15.50	−44.2617	–	–	–

characterized by its mean value, i.e. the distribution of individual θ ranges mainly from 20° to 100°. This high dispersion could be explained by: (i) an intrinsically more complex θ distribution, such as a bimodal distribution like the one suggested by Goodman et al. (1990) for the Perseus complex; or (ii) the fact that the magnetic field did not play a major role in determining the cloud structure at small scales.

Andreazza & Vilas-Boas (1996) pointed out that the distribution of the magnetic field orientation does not have any apparent relationship with either the major axis of the condensations or the filaments. We tested these conclusions by observing the relative orientation of the mean polarization angles of the stars located in projection very close to the condensations in both filaments. Based on the results obtained, the magnetic field in Lupus 1 appears to be highly variable from one condensation to another and even inside the same condensation: the polarization angles are 17° (stars 4 and 6) or 100° (stars 5 and 7) for the condensation A, 55° for condensation D, and 23° (stars 23 and 27) or 75° (stars 24, 25, 26, 28 and 31) for the joined condensations E–F. In contrast, the polarization vectors in Lupus 4 appear highly collimated: average values of 25°, 22°, 23°and 28° are obtained for condensations A to D. These facts, along with the features found from our CO profiles (line asymmetries, broad profiles and double-peak structures) could indicate that Lupus 1 has a more intricate cloud structure than Lupus 4.

4.4 Molecular gas motion

In order to illustrate both the velocity field and the distribution of the molecular material in Lupus 1, we have analysed three subsets of

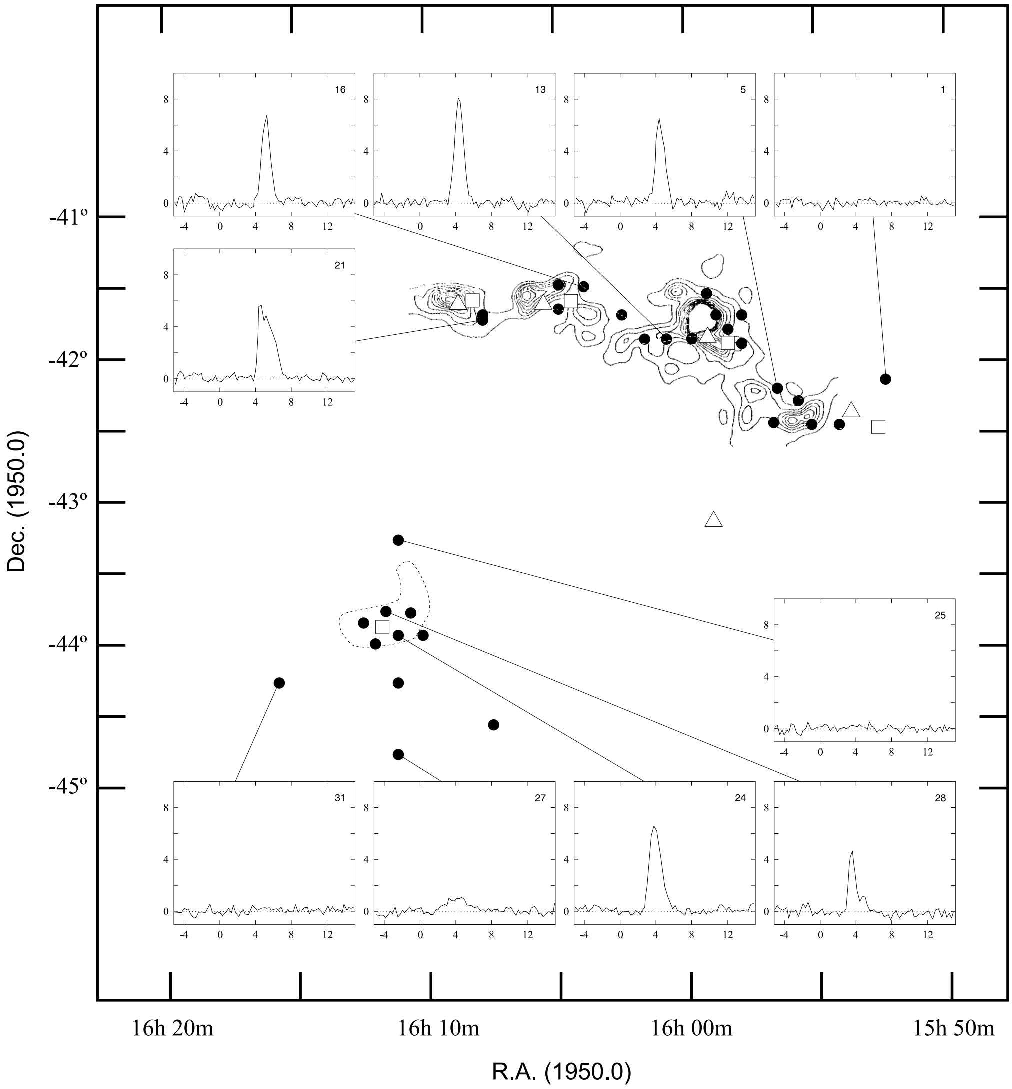

Figure 5. The same as Fig. 4 for the Lupus 4 region. Dark points correspond to the CO observations reported in this paper. The open squares indicate the H_2CO positions observed by Sandqvist & Lindroos (1976), and the triangles indicate the H_2CO observations of Goss et al. (1980). In the filament, contour lines are from the visual absorption map of Andreazza & Vilas-Boas (1996), while the dashed line in the globule represents the optically defined outer boundary of the dark cloud.

CO data: (1) along the major axis of the optical filament (subset A); (2) along a declination of $\approx -34\overset{\circ}{.}25$ (subset B); and (3) along a declination of $\approx -33\overset{\circ}{.}5$ (subset C). Figs 8(a) to (c) show the variations of the mean temperature-weighted radial velocity, V_R, across each subset. Along the filament, the velocity varies from ~ 6 km s^{-1} towards the north-west down to 4 km s^{-1} to the south-east. The two 'transverse cuts' (subsets B and C) exhibit velocity gradients, quite evident in subset B, increasing from west to east. The H_2CO velocities measured by Sandqvist & Lindroos (1976), shown in Fig. 8 as open circles, agree with the trend shown by our CO measurements.

Fig. 9 shows the changes in V_R along the Lupus 4 filament. The radial velocity reaches a minimum of ≈ 4 km s^{-1} towards the central part of the filament. It could be indicating the presence of a small expansion or contraction in the cloud. Fig. 9 also includes the H_2CO measurements of Sandqvist & Lindroos (1976) and Goss et al. (1980). The agreement between both data sets is quite good.

All measured velocities in GF18 are in the narrow range from 3.5 to 4 km s^{-1}, slightly lower than the corresponding ones for Lupus 4 itself. In addition, a systematic asymmetry in all CO profiles was noticed: V_R is always greater than the peak velocity, suggesting the presence of a low-intensity component at higher velocities (see Fig. 5).

A crude one-dimensional model aimed at studying the dynamical stability of the clouds was constructed for both filaments. We have considered each filament as a bunch of aligned condensations moving at different velocities along the line of sight. This simple-minded model shows that Lupus 1 would not be recognizable as a single cloud after 3 or 4 Myr. In constrast, Lupus 4 would keep its actual morphology for at least 5 Myr.

Table 4. Mean polarization angles in Lupus 1 and Lupus 4.

Regions	Mean angle (°)	Std. deviation (°)
Close stars — Lupus 1	52	23
Close stars — Lupus 4	26	9
Field stars — Lupus 1	126	25
Field stars — Lupus 4	174	24

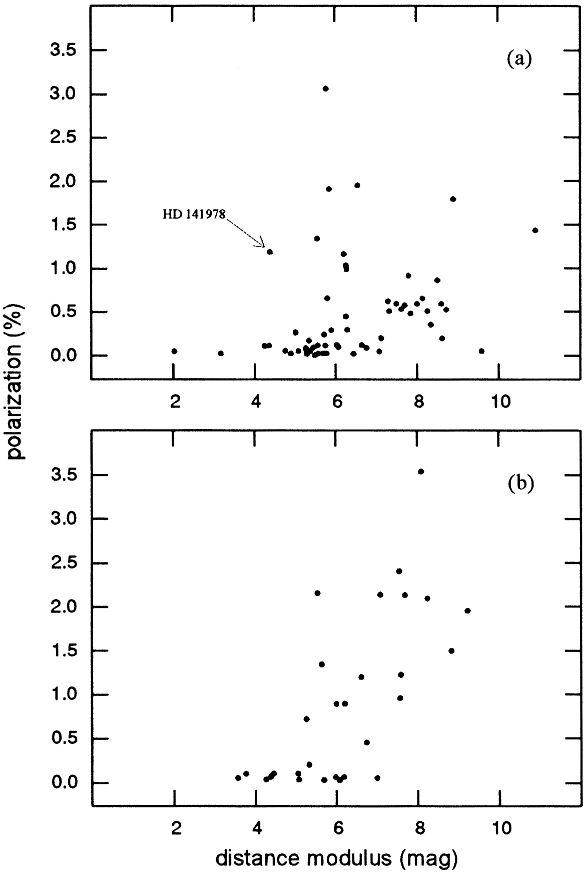

Figure 6. Percentage polarization versus extinction-corrected distance modulus from (a) Lupus 1 and (b) Lupus 4. The position of HD 141978 is indicated; see discussion in Section 4.1.

4.5 Relation to Gould's Belt

The distances derived from our polarization observations (125–140 pc) are in good agreement with those derived by other authors (130–170 pc), indicating that both filaments belong to the local

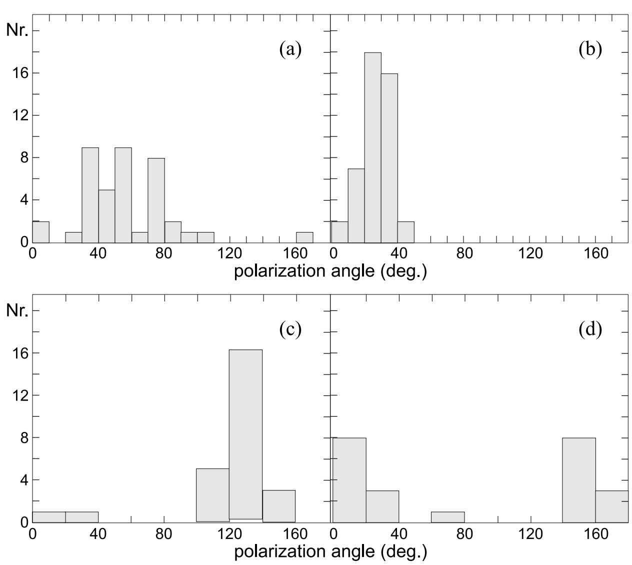

Figure 7. Number distributions of the polarization angle for (a) Lupus 1; (b) Lupus 4; (c) Lupus 1 'field stars'; and (d) Lupus 4 'field stars'.

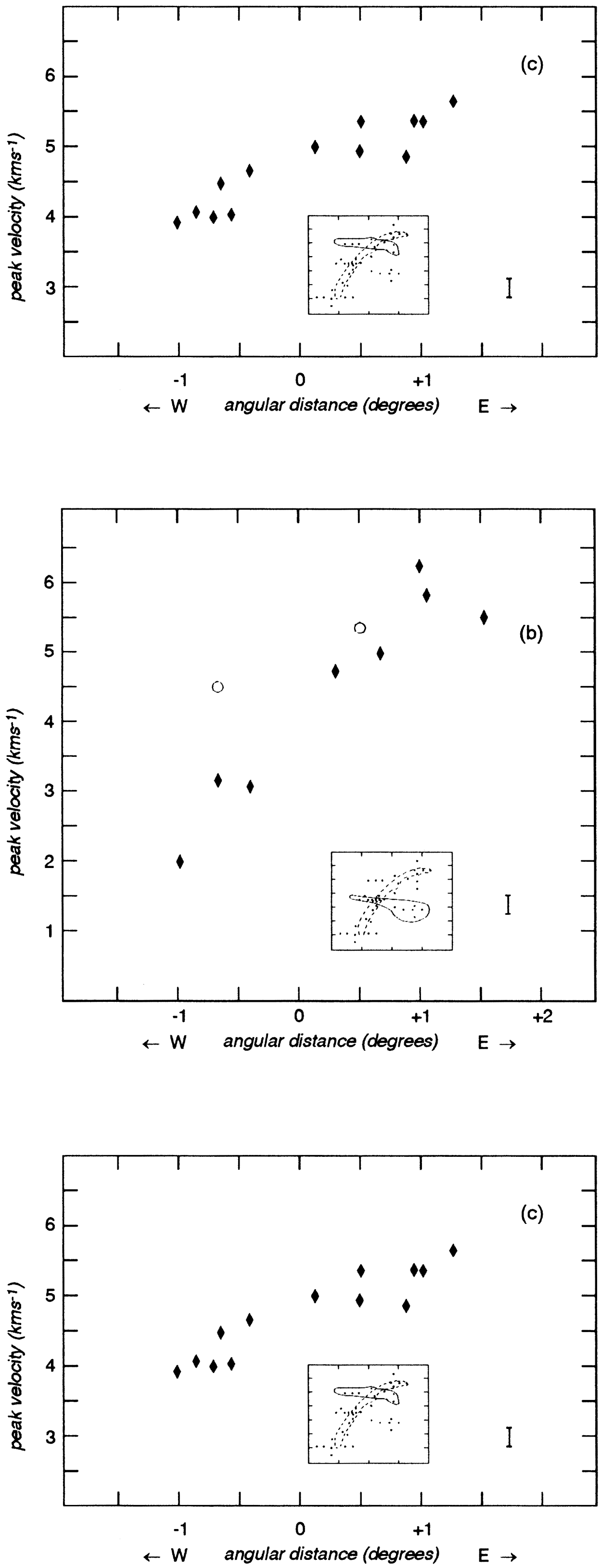

Figure 8. Variation of the ^{12}CO peak velocity along the Lupus 1 filament. Error bars are shown in the right bottom corner of each figure. The small figures given in the lower part sketch the approximate positions of the considered profiles. Zero-offset positions (RA, Dec.) of each subset are: (a) (15^h40^m, $-34°$); (b) (15^h40^m, $-33\overset{\circ}{.}5$); (c) (15^h40^m, $-34\overset{\circ}{.}5$).

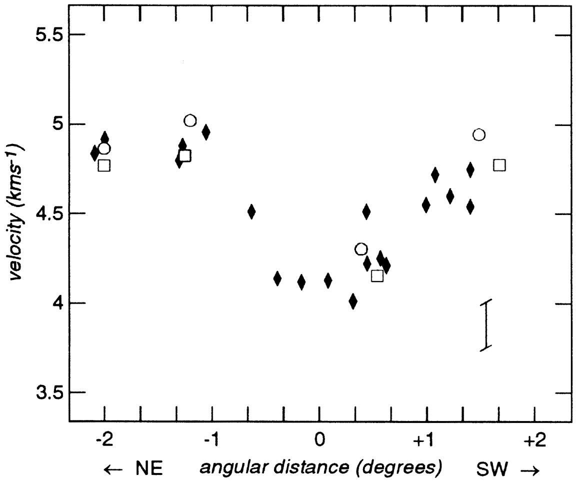

Figure 9. Variation of the ^{12}CO peak velocity along the Lupus 4 filament. An error bar is shown in the right bottom corner. The zero-offset position is (RA, Dec.) = (16^h00^m, $-41\overset{\circ}{.}858$).

interstellar medium. The mean radial velocities derived from both the CO and the H_2CO data are consistent with the outward peculiar motion of the H I, dust clouds and bright young stars outlining the local system called Gould's Belt (Lindblad et al. 1973; Olano 1982; Pöppel 1997).

5 CONCLUSIONS

From the starlight polarization data we estimated a lower distance limit of 140 and 125 pc for Lupus 1 and Lupus 4, respectively.

The magnetic field towards Lupus 4 has a well-defined direction, which coincides with the magnetic field direction inferred from the 'field stars' data. This field is almost perpendicular to the major axis of the cloud.

Close to Lupus 1 the magnetic field direction seems to change from place to place without exhibiting a clear pattern. The major axis of this cloud is parallel to the magnetic field direction derived from the 'field stars'.

The radial velocity derived from molecular line data, and the distance determination of these clouds, seems to indicate that they belong to Gould's Belt.

ACKNOWLEDGMENTS

We wish to thank all the staff of the Complejo Astronómico El Leoncito (CASLEO) for their hospitality and invaluable help with the polarimetric observations. We also wish to thank Dr. C. López, from the Félix Aguilar Observatory, for his collaboration with us in taking the optical plates. One of us (EMA) is very much indebted to Drs R. Cohen and P. Thaddeus for having allocated, a long time ago, observing time at the Columbia Southern Millimeter-Wave Facility at Cerro Tololo, Chile. This work was partially supported by the Argentinian National Research Council (CONICET) under project PID 3-0838800/88.

REFERENCES

Andreazza C. M., Vilas-Boas J. W. S., 1996, A&AS, 116, 21
Appenzeller I., Mundt R., Wolf B., 1978, A&A, 63, 289
Arnal E. M., Morras R., Rizzo J. R., 1993, MNRAS, 265, 1
Cohen R. S., 1983, in Burton W., Israel F.P., eds, Survey of the Southern Galaxy. Reidel, Dordrecht, p. 265
Corbally C. J., Garrison R. F., 1984, in Garrison C. J., ed., MK Process and Stellar Clasification. David Dunlap Observatory, University of Toronto, p. 277
Davis L., Greenstein J. L., 1951, ApJ, 114, 206
Franco G. A. P., 1990, A&A, 227, 499
Goodman A. A., Bastien P., Myers P. C., Ménard F., 1990, ApJ, 359, 363
Goss W. M., Manchester R. N., Brooks J. W., Sinclair M. W., Manefield G. A., Danziger I. J., 1980, MNRAS, 191, 533
Heiles C., Goodman A. A., McKee C. F., Zweibel E. G., 1993, in Levy E. H., Lunine J. I., eds, Protostars and Planets III. Univ. Arizona Press, Tucson, p. 279
Heyer M. H., Vrba F. J., Snell R. L., Schloerb F. P., Strom S. E., Goldsmith P. F., Strom K. E., 1987, ApJ, 321, 855
Hiltner W. A., 1956, ApJS, 2, 389
Houk N., Cowley A. P., 1975, in Michigan Catalogue, Two–dimensional Spectral Types for the HD Stars. University of Michigan, Ann Arbor, Michigan
Hughes J., Hartigan P., Clampitt L., 1993, AJ, 105, 571
Krautter J., 1991, in Reipurth B., ed., Low Mass Star Formation in Southern Molecular Clouds, ESO Scientific Report No. 11, p. 127
Krautter J., Wichmann R., Schmitt J. H. M. M., Alcalá J. M., Neuhäuser R., Terranegra L., 1997, A&AS, 123, 329
Lindblad P. O., Grape K., Sandqvist A., Schober J., 1973, A&A, 24, 309
Lynds B. T., 1962, ApJS, 7, 1
Magalhaes A. M., Benedetti E., Roland E. H., 1984, PASP, 96, 383
Morras R., 1981, AJ, 86, 875
Murphy D. C., Cohen R., May J., 1986, A&A, 167, 234
Myers P. C., Goodman A. A., 1991, ApJ, 373, 509
Olano C. A., 1982, A&A, 112, 195
Pöppel W. G. L., 1997, Fund. Cosmic Phys., 18, 1
Ramana Murthy P. V., Wolfendale A. W., 1993, in Carswell R. F., Lin D. N. C., Pringle J. E., eds, Gamma Ray Astronomy. Cambridge Univ. Press, Cambridge, p. 137
Sandqvist A., Lindroos K. P., 1976, A&A, 53, 179
Schneider S., Elmegreen B. G., 1979, ApJS, 41, 87
Schwartz R. D., 1977, ApJS, 35, 161
Serkowski K., 1974, in Carleton N., ed., Methods of Experimental Physics, 12, Part A. Academic Press, New York, p. 361
Strom S. E., Strom K. E., Edwards S., 1988, in Pudritz R., Fich M., eds, Galactic and Extragalactic Star Formation. Kluwer, Dordrecht, p. 53
Strong A. W. et al., 1988, A&A, 207, 1
Shu F. C., Adams F. C., Lizano S., 1987, ARA&A, 25, 23
Vrba F. J., Rydgren A. E., 1984, ApJ, 283, 123
Vrba F. J., Strom S. E., Strom K. M., 1976, AJ, 81, 958